Wiley
Advances in Civil Engineering
Volume 2024, Article ID 6314144, 13 pages
https://doi.org/10.1155/2024/6314144

WILEY

Research Article

Low-Cost Portable Road Smoothness Testing Method Based on Pseudo-Vibration Velocity Range

Hongwei Jiang,[1] Xinlong Tong,[1] Yanhong Zhang,[1] Zhoujing Ye,[2] Junqing Li,[2] Yu Wang,[3] and Yinghao Miao[2]

[1]*China Highway Engineering Consulting Group Company Ltd., Beijing 100089, China*
[2]*National Center for Materials Service Safety, University of Science and Technology Beijing, Beijing 100083, China*
[3]*Central Expressway Management (Shanxi) Co., Ltd., Taiyuan 030000, Shanxi Province, China*

Correspondence should be addressed to Xinlong Tong; maniga@163.com and Yinghao Miao; miaoyinghao@ustb.edu.cn

Received 5 August 2023; Revised 2 February 2024; Accepted 29 March 2024; Published 27 May 2024

Academic Editor: Chayut Ngamkhanong

Road smoothness not only directly affects the safety and comfort of vehicle travel but also relates to the efficiency and cost-effectiveness of road maintenance. Traditional road smoothness detection methods usually require professional equipment and personnel, leading to high costs and cumbersome operations. Therefore, finding a low-cost, simple, and accurate method for detecting road smoothness is of great significance. This study uses vehicle-mounted acceleration sensors to detect road smoothness, establishing a correlation between driving vibration acceleration data and the international roughness index (IRI). For this research, a driving vibration acceleration data acquisition device was developed, and the driving acceleration data from the test sections were denoised and their feature values extracted. The pseudo-vibration velocity range was used as the characteristic index representing the road surface smoothness IRI value. Testing with different vehicle types showed that the method is applicable to both sedans and SUV models, yielding a relative error of 8.9% for the sedan smoothness test model and 6.7% for the SUV smoothness test model. This study contributes to conducting large-scale road smoothness detection at a low cost, improving the efficiency of road maintenance and operations.

1. Introduction

Roads serve as crucial transportation infrastructure, fulfilling people's basic travel needs, and ensuring transportation efficiency. However, roads inevitably deteriorate due to vehicle loads and environmental factors, making timely maintenance essential. Given that road maintenance budgets are often limited, prioritizing which roads need maintenance is of utmost importance [1, 2]. This requires real-time monitoring of road surface quality.

Road surface evenness detection can provide insights into the condition of the road surface, and vehicle-mounted laser rangefinders are commonly utilized for this purpose. Urano demonstrated that point clouds recorded by a laser scanner mounted on an autonomous vehicle can be used to extract transverse road contours, offering a cost-effective method for preliminary road surface evenness investigations and identifying areas requiring detailed inspection [3, 4, 5]. Bennett introduced a precise rut depth measurement system using laser technology, providing an accurate measurement scheme [6].

However, current methods for detecting road surface evenness face significant challenges. They require the use of expensive, specialized equipment that demands intricate calibration by trained personnel. Furthermore, these methods often necessitate specific equipment mounted on vehicles, limiting their wider applicability. Typically conducted on an annual basis, these assessments are costly and inefficient. Consequently, extending these techniques to lower grade roads, particularly in rural areas, is problematic. The high costs, complex calibration processes, and dependence on specialized vehicle-mounted equipment hinder regular, cost-effective evenness assessments, especially for rural road networks. To address these issues, researchers proposed portable road surface evenness detection devices based on driving acceleration, using low-cost acceleration data collection devices

on small vehicles to assess road conditions through driving acceleration data collection and processing. The vibration signal contains a lot of information, which can be used for road surface evenness detection and structural health monitoring [7, 8].

Various studies have explored road surface evenness and damage detection using different techniques. Accelerometer-based indices calculation methods include Tomiyama and Kawamura's [9] lifting wavelet transform (LWT) method using vehicle axle accelerometers, Chen et al.'s [10] indices related to evenness, Brunauer et al.'s [11] RSCI index reflecting road bumpiness and abnormalities, and Zhang et al.'s [12] three-axis vibration acceleration data collection using cushion-type accelerometers with a GA-BP neural network. Machine learning models for damage estimation involve Chatterjee and Tsai [13] RNNs with long short-term memory units using 3D pavement data, and Zhang et al. [14] CrackNet, a CNN-based model for asphalt pavement crack detection. Regression models for road condition assessment encompass Elhadidy et al.'s [15] simplified regression model using the LTPP database, Aleadelat's [16] correlation models between PSI and variance of the smoothed signal, and Hafez et al.'s [17] univariate regression multivariate imputation model using historical PMS data. The smartphone-based monitoring systems mentioned include Zang et al.'s algorithm [18], which identifies potholes and humps using smartphones mounted on bicycles. The projects Nericell, Roadroid, and SmartRoadSense [19, 20, 21], which offer web-based GIS platforms for visualizing results of road surface evenness detection. Finally, Abdelaziz [22] developed a flexible pavement IRI prediction model using the LTPP database, multivariate linear regression analysis, and ANNs, achieving a correlation coefficient (R^2) value of 0.75 for IRI prediction. Zhang et al. [23] developed a client application installed on smartphones, establishing a relationship between acceleration, international roughness index (IRI), and longitudinal profile elevations through theoretical formula derivation. The IRI calculated by this theoretical method is close to that calculated by digital survey vehicles, with a maximum relative error of less than 10%, enabling various vehicles to be used for road roughness evaluation. Xu and Yu [24] proposed a real-time road surface evenness recognition method based on a lightweight residual convolutional network and time-series acceleration, achieving a classification accuracy of up to 98.7% for road surface evenness. This significantly improves the accuracy of recognition algorithms and reduces computational demands, making it suitable for classifying road surface evenness levels.

Douangphachanh and Oneyama [25] mounted two Android smartphones and a GPS recorder on a Toyota VIGO pickup and a Toyota Camry sedan, testing surface evenness in the range from 1.5 to 16 m/km at speeds of 10–80 km/hr. They found a correlation coefficient of 0.67–0.75 between IRI and acceleration, demonstrating that vehicle type and equipment have a minor impact on results. Bisconsini et al. [26] mounted a Samsung Galaxy S5 mini smartphone, equipped with an accelerometer and GPS, in a standard passenger car. They tested surface evenness in the range of 1–16 m/km at speeds of 20–60 km/hr, finding a correlation between IRI and acceleration of 0.97–0.99, with the speed of measurement having no significant impact on evenness assessments. Aleadelat et al. [27] collected IRI data from 35 road sections at two different speeds (40 and 50 miles per hour) and converted the recorded acceleration into MATLAB software variables. The results showed that the coefficient of determination (R^2) between RMS and standard IRI at the two speeds (40 and 50 miles per hour) was 0.83 and 0.86, respectively. According to the model constructed by Alatoom and Obaidat [28], the correlation coefficient R^2 between normalized root mean square, normalized variance (NVAR) of the Z-axis acceleration, and IRI is 0.69, which requires further optimization. Aboah and Adu-Gyamfi [29] established three predictive models to correlate with actual road surface IRI, with the model developed using deep learning achieving an R^2 of 0.79. However, the sample size for model construction was small (only 36), making it difficult for the model to interpret large datasets. Sandamal and Pasindu [30] examined the ability of a smartphone application (Roadroid) to estimate IRI on rural road surfaces. The results showed good accuracy ($R^2 = 0.77$) in IRI measurement using Roadroid, compared to IRI measured by a Bump Integrator device. Xu et al. [31] developed a portable road surface evenness detection device, PRD, using the Arduino platform for data collection, and constructed an RFR model for immediate IRI prediction, achieving an R^2 of 0.967 in the test set when combined with subsequent data analysis. Bidgoli et al. [32] developed an automated system for the immediate collection of road evenness data. This system was tested on a secondary road, comparing its data with those from a road surface profiler device. The results showed a high correlation ($R^2 = 0.85$) between the two methods. Du et al. [33] collected data by installing a self-designed vehicle-mounted sensor terminal in a sedan and SUV, driving at non-uniform speeds, achieving a final fit of $R^2 = 0.87$.

This study aims to address the issues present in current road surface evenness detection methods, such as the need for expensive equipment, specialized personnel, and complex equipment calibration procedures. Although there have been developments in portable road surface evenness detection devices and data processing methods, there is still a need for further optimization of algorithms and models. Against this backdrop, we propose a road surface evenness testing method based on driving vibration acceleration. This method not only reduces equipment costs but also employs a simple linear fitting model more suited to engineering applications.

Our method is characterized by its low cost, simplified operation, strong applicability, and capability for large-scale rapid testing. Compared to traditional methods, our approach uses low-cost equipment, avoiding the need for expensive investments and thus reducing the overall cost of testing. By relying on driving vibration acceleration for testing, it eliminates the need for specialized personnel, simplifying the operation and obviating the need for complex equipment calibration. The use of a simple linear fitting model aligns more closely with the practical needs of engineering applications, offering higher applicability and operability. Additionally, our method enables large-scale rapid testing, providing more efficient technical support for road maintenance management. Overall, this new method based on driving vibration acceleration offers a more economical, practical, and rapid solution for road surface evenness detection.

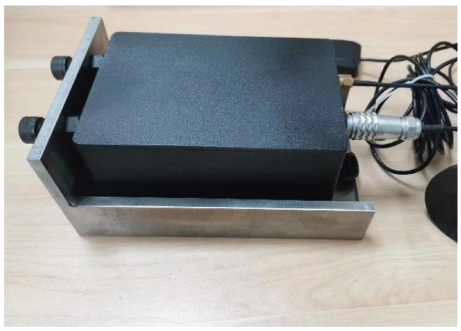

Figure 1: Driving vibration acceleration data collection device.

2. Driving Vibration Data and IRI Data Collection

2.1. Test Equipment Development. Using a self-developed driving vibration acceleration data collection device for data collection, the device can simultaneously collect three-axis acceleration (*X*-, *Y*-, *Z*-axis), GPS coordinates (latitude and longitude), and vehicle speed while keeping all the information time-synchronized, as shown in Figure 1.

The collection frequency of the accelerometer is 1,000 Hz, and the model of the accelerometer is ADXL355. Its sensitivity is 400 mV/g, and the resolution is 0.65 mg. The GPS uses a u-blox module, a high-performance global positioning system component, with an output frequency of 10 Hz and a positioning performance of less than 2.5 m. The device is connected to a computer via WiFi, and the acceleration data can be displayed in real-time on the software interface. The device can be fixed on the test vehicle using magnetic suction or a custom fixed slot.

2.2. Test Plan Design. In order to measure the road surface evenness and corresponding driving acceleration data, the driving vibration acceleration data collection device is installed on a CICS vehicle. A fixed slot is fabricated for easy installation and removal, and it is rigidly connected to the vehicle using bolts on site. The driving vibration acceleration data collection device is placed in the fixed slot and fixed with suction cups at the bottom, as shown in Figure 2.

In order to ensure that the experimental process is as free from interference as possible and to ensure the accuracy of the test results, three sections of asphalt road on Shuinan Road in Changping District, Beijing, were selected for testing. These are six sections: 1–1, 1−2, 2–1, 2−2, 3–1, and 3–2. The traffic and pedestrian flow in these sections is relatively low, and the degree of road surface damage varies, making them representative. The total length of the road is 14 km, and it is a two-way, four-lane first-class highway, as shown in Figure 3.

After controlling the vehicle speed between 40 and 60 km/hr, simultaneously press the collection buttons on both devices to start measuring the road surface data of the same lane. At the same time, record the speed and driving conditions during the measurement. The *X*-axis direction is aligned with the longitudinal direction (driving direction), the *Y*-axis direction is the transverse direction, and the *Z*-axis direction is the vertical direction. The *Z*-axis acceleration data are used for analysis.

2.3. Test Data Collection

2.3.1. IRI Data for the Test Sections. Once the IRI values are collected using the CICS vehicle, it is essential to align these values with the driving vibration acceleration data based on distance, while eliminating sections where lane changes and traffic lights occur during data collection. Following the data organization, the IRI (10 m) values for the test sections are illustrated in Figure 4.

Figure 4 shows the measured IRI values for the six sections: 1–1, 1–2, 2–1, 2–2, 3–1, and 3–2. As can be seen from the figure, the IRI values for each section vary significantly, and the selected sections have noticeable differences in road surface evenness. This represents different road surface damage conditions.

2.3.2. Acceleration Data for Test Sections. In order to facilitate the observation of the relationship between IRI values and driving vibration acceleration, and to ensure proper data alignment based on driving distance, the average driving vibration acceleration is calculated. According to the IRI value for every 10 m, when driving at a constant speed of 40 km/hr, the average value needs to be calculated every 900 ms. Figure 5 shows the driving vibration acceleration values for Section 1–1 before and after averaging.

From Figure 5, it can be seen that the driving vibration acceleration data collection equipment collects uniform noise fluctuations, but on uneven road surfaces, there will be significant peaks and valleys, indicating that the vehicle is experiencing vibrations, and the vibration signals are more pronounced than the noise signals. The driving vibration data fluctuates within a certain range, and the relationship between road surface evenness and driving vibration can be analyzed by comparing the IRI data based on the difference and frequency of peaks and valleys.

3. Relationship Model between Driving Vibration Feature Index and IRI

3.1. Pseudo-Vibration Acceleration Data Conversion. After fitting the synchronized acceleration data with IRI values, the standard deviation, range, and sum of absolute values with the highest fitting degree were selected for subsequent feature index calculation. Let the acceleration data be $A = (a_1, a_2, \ldots, a_n)$, n is the number of sampling points; a_i is the acceleration (mg) of the i sampling point; and the arithmetic mean of the acceleration of the sampling points (mg). The calculation methods of the indicators are as follows:

$$m = \frac{1}{n}\sum_{i=1}^{n} a_i, \tag{1}$$

$$\sigma = \sqrt{\frac{1}{n}\sum_{i=1}^{n}(a_i - m)^2}, \tag{2}$$

where σ is the standard deviation (SD).

$$\text{Range} = \max(A) - \min(A), \tag{3}$$

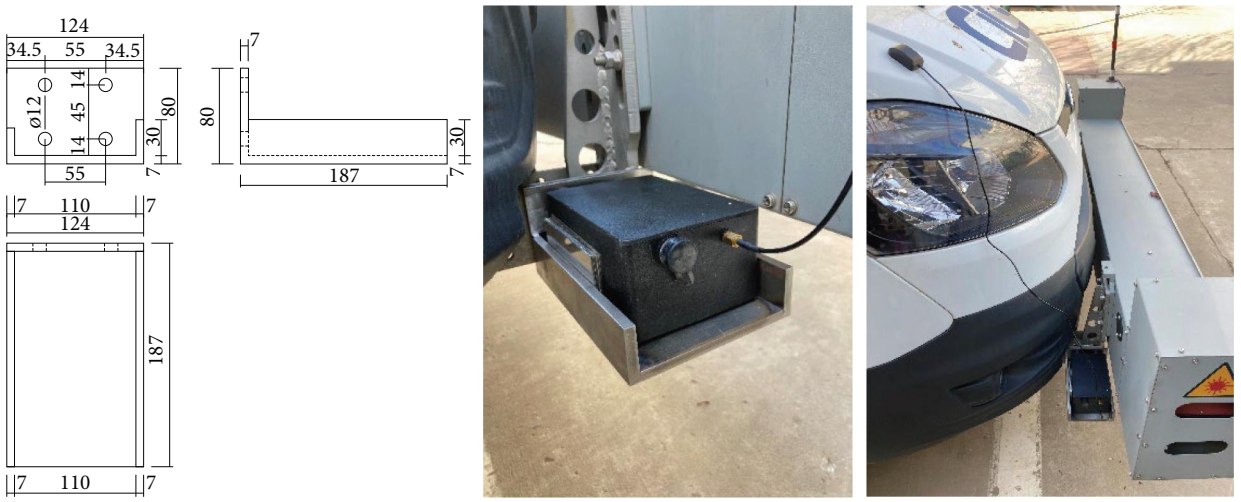

Figure 2: Driving vibration acceleration data collection device installed on a CICS vehicle.

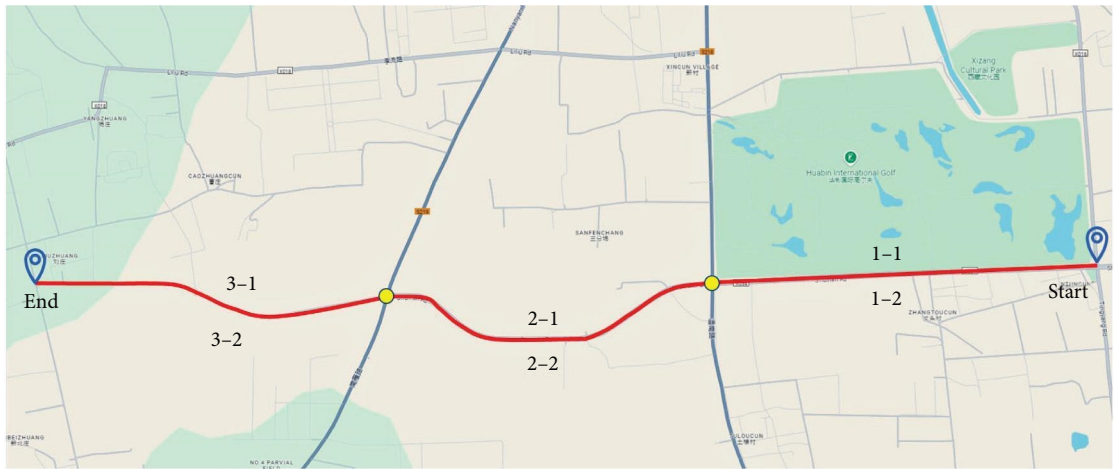

Figure 3: Schematic diagram of the selected test sections.

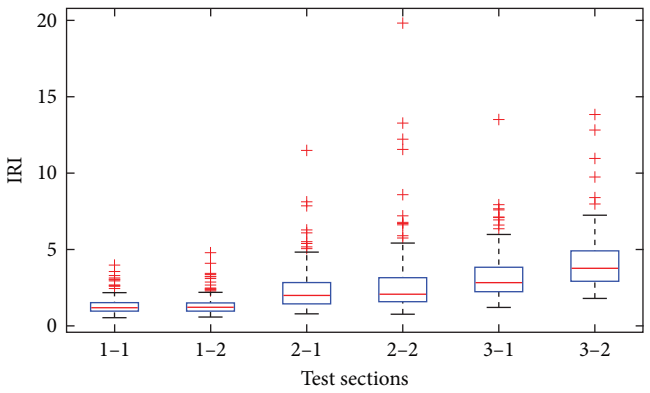

Figure 4: IRI values of the test sections (10 m).

where Range is the range.

$$\text{Sum}_{\text{abs}} = \sum_{i=1}^{n} |a_i|, \tag{4}$$

where Sum_{abs} is the sum of absolute values.

To make the driving vibration data fit better with the IRI and establish a more accurate road surface evenness calculation model, pseudo-vibration velocity is innovatively used to transform the acceleration data. The specific conversion process is as follows:

$$V_1 = 0 + a_1, \tag{5}$$

$$V_2 = V_1 + a_2, \tag{6}$$

$$V_3 = V_2 + a_3, \tag{7}$$

$$V_n = V_{n-1} + an. \tag{8}$$

Form the pseudo-vibration velocity $A' = (V_1, V_2, \ldots, V_n)$, adjust A in the above feature index to A', and adjust ai to V_i. Calculate the feature index using pseudo-vibration velocity.

By accumulating acceleration to obtain pseudo-vibration velocities, it becomes easier to understand the changes in velocity experienced by a vehicle within a unit of time.

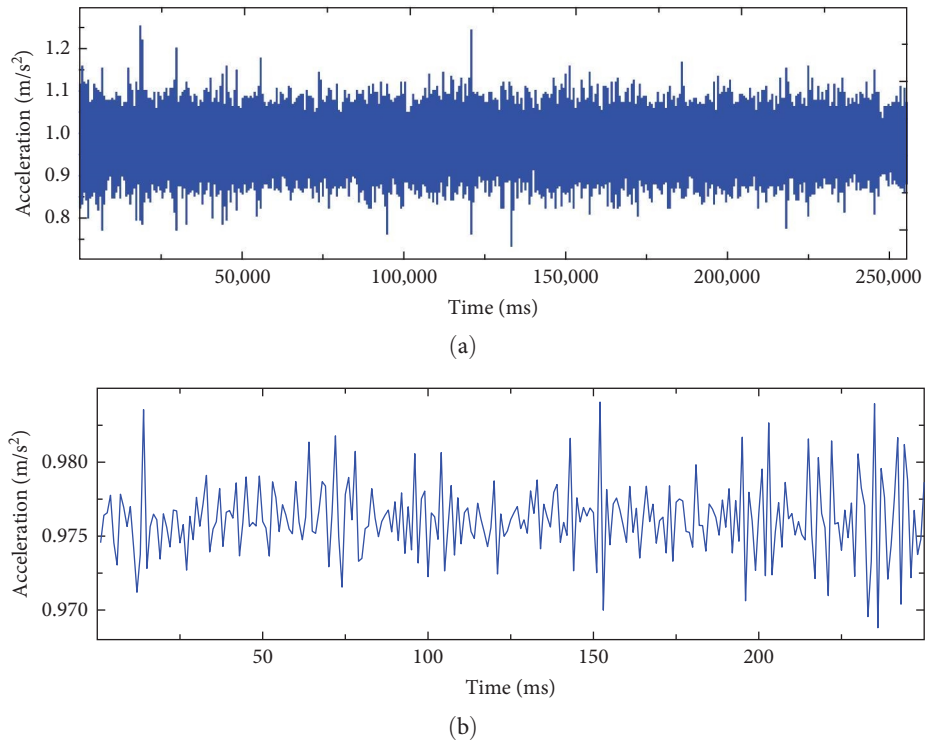

Figure 5: The driving vibration acceleration values for Section 1–1 before (a) and after (b) averaging.

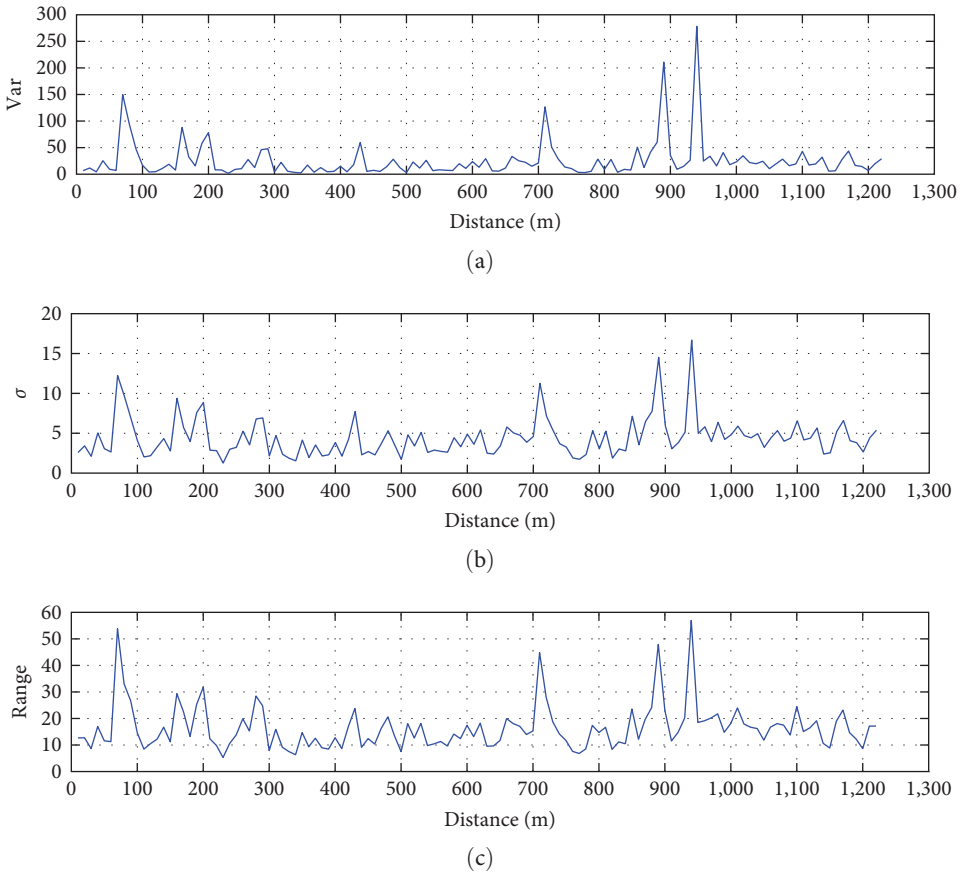

Figure 6: Vibration amplitude index calculated with pseudo-vibration velocity (10 m calculation unit). (a) Pseudo-vibration velocity processing acceleration signal. (b) Standard deviation processing acceleration signal. (c) Range processing acceleration signal.

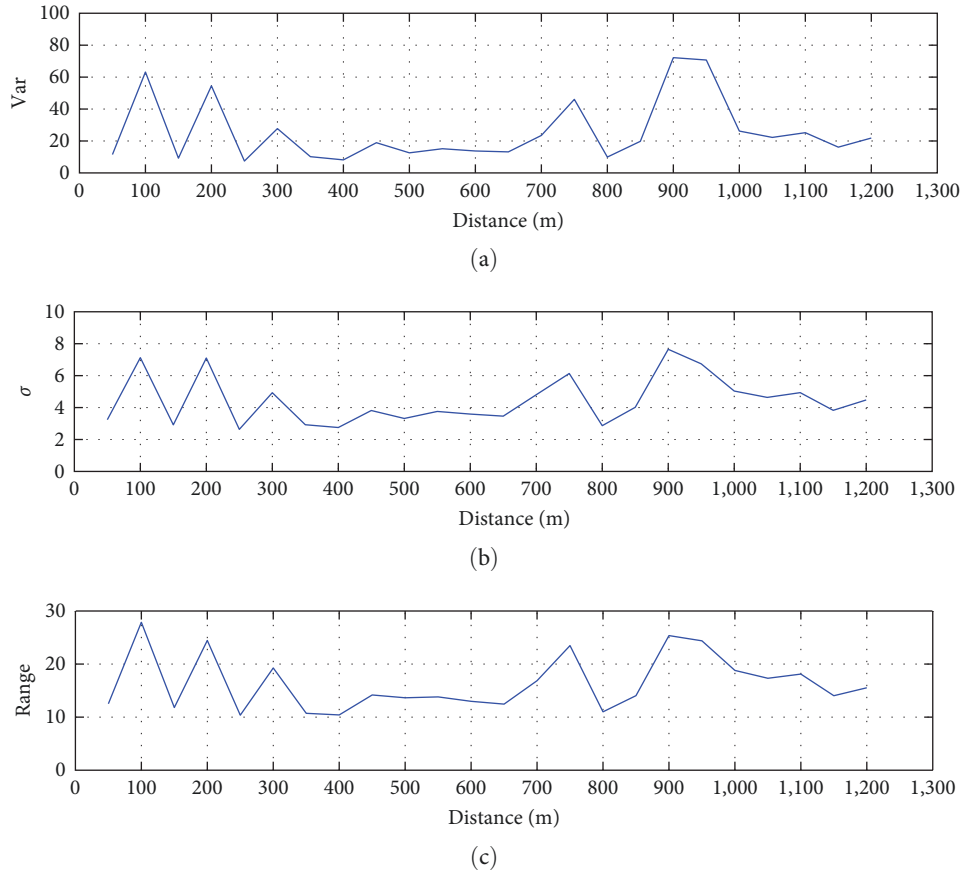

Figure 7: Vibration amplitude index calculated with pseudo-vibration velocity (50 m calculation unit). (a) Pseudo-vibration velocity processing acceleration signal. (b) Standard deviation processing acceleration signal. (c) Range processing acceleration signal.

This helps to more intuitively depict the vehicle's vibrations on the road. At the same time, the process of accumulating acceleration to obtain pseudo-vibration velocities can simplify the model to some extent, making the calculation of characteristic indicators more straightforward and reducing the complexity introduced in the computational process. Finally, by using accumulated pseudo-vibration velocities, it may be possible to better capture the cumulative effect of vehicle vibrations on the road, thereby more comprehensively reflecting the road surface evenness, especially in cases of long-duration driving.

The term "pseudo-vibration velocities" is used to better describe the method of calculating vibration velocity, which is obtained by accumulating acceleration. The use of "pseudo-vibration velocities" emphasizes that this is a velocity derived from the accumulation of vibration, not the actual velocity of the object. It highlights the difference between vibration velocity and real velocity, rather than directly measured velocity.

3.2. Feature Index Calculation Based on Pseudo-Vibration Velocity. Using 10, 50, and 100 m as calculation units, the feature index calculation and analysis of pseudo-vibration velocity data were performed. The pseudo-vibration velocity amplitude variance (Var), standard deviation (SD), and range (Range) were selected as the objects of analysis.

The calculation feature index with a 10 m calculation unit is shown in Figure 6. These feature indexes have high similarity in amplitude peaks during vehicle driving.

Figure 6(a) shows the results of processing the vibration amplitude signal using pseudo-vibration velocity (Var). In the 0–100, 700–800, and 850–950 m sections, there are four relatively prominent peaks in vehicle amplitude. This indicates that in these sections, the vehicle has a larger vibration, the road surface evenness is worse, and it has a negative impact on vehicle driving. Figure 6(b) shows the results of processing the vibration amplitude signal using the standard deviation (SD). Although there are also significant peaks in the same four sections, there are more interference peaks, which affect the accurate determination of the uneven road section's position. Figure 6(c) shows the results of processing the vibration amplitude signal using the range (Range), and these prominent sections are still within the four areas mentioned earlier. In summary, when using a 10 m calculation unit, the pseudo-vibration velocity, standard deviation, and range can better express the similarity in processing road surface vibration amplitude, and can more accurately reflect the relationship between vibration amplitude and road surface evenness within the test section.

Using pseudo-vibration velocity as the base data and 50 m as the calculation unit, the feature index calculation is shown in Figure 7. From Figure 7, it can be seen that for

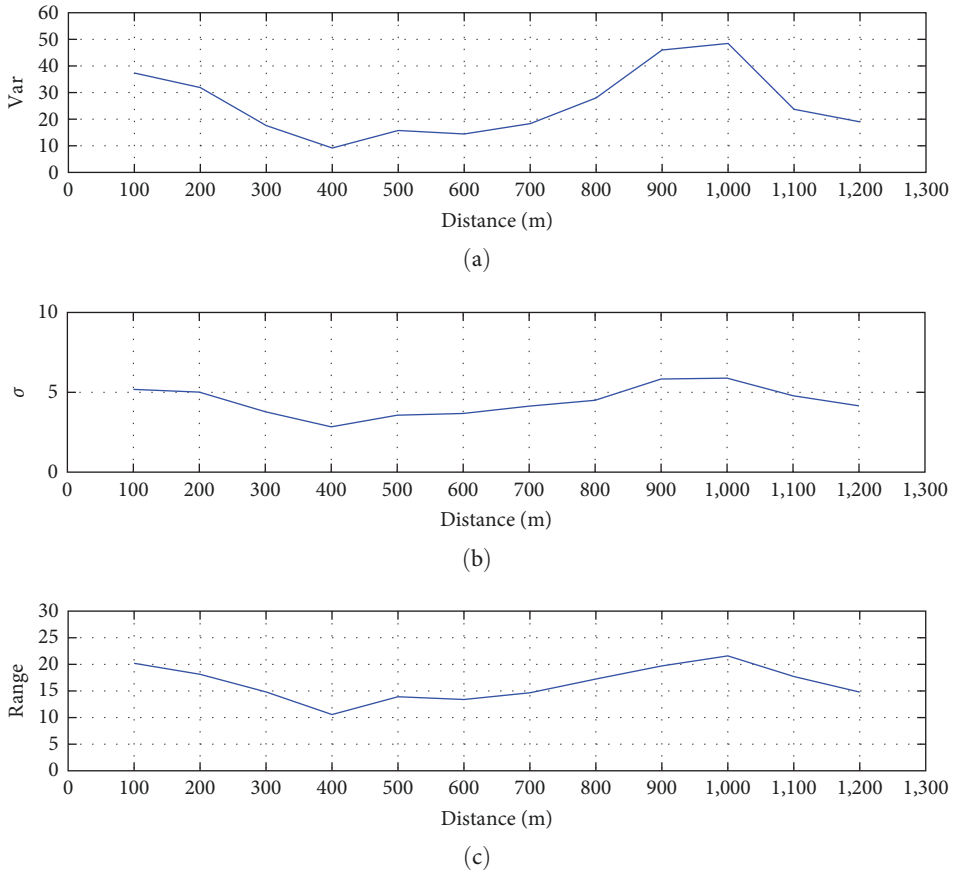

Figure 8: Vibration amplitude index calculated with pseudo-vibration velocity (100 m calculation unit). (a) Pseudo-vibration velocity processing acceleration signal. (b) Standard deviation processing acceleration signal. (c) Range processing acceleration signal.

Table 1: Fitting results of V Range and IRI when the vehicle is driving at a uniform speed of 40 km/hr.

IRI (m)	10	20	30	40	50	60	70	80	90	100
R^2	0.234	0.400	0.511	0.663	0.754	0.663	0.696	0.752	0.814	0.873
a	0.078	0.109	0.117	0.137	0.146	0.126	0.136	0.154	0.151	0.161
b	1.812	1.290	1.151	0.825	0.673	0.989	0.820	0.530	0.587	0.423

different feature indicators (pseudo-vibration velocity, standard deviation, range), the vibration amplitude during vehicle driving is basically consistent. There are more noticeable peaks in the 100, 200, 300, 700–800, and 900–1,000 m sections. When calculating the feature value with a 50 m calculation unit, the road surface evenness displayed using the above three feature indicators is approximate in overall trend, and the peak positions are almost coincident. Compared to the 10 m calculation unit, the 50 m calculation unit has a wider applicability in expressing road surface evenness.

Using pseudo-vibration velocity as the base data and 100 m as the calculation unit, the feature index calculation is shown in Figure 8. For different feature indicators (pseudo-vibration velocity, standard deviation, and range), the trend of vibration amplitude during vehicle driving is similar, and there is a more noticeable peak near 1,000 m, indicating that the vehicle's vibration amplitude is larger, and the road surface evenness becomes worse within this range. When using a 100 m calculation unit to calculate the feature value, the vibration amplitude is almost a straight line in the parts where the road surface evenness changes slightly, and it has a significant display for the parts where the road surface evenness is worse, making the sections that need maintenance more prominent.

In summary, when using the same calculation unit to calculate the feature index, the vibration amplitude is basically consistent during vehicle driving for different feature indicators, and the consistency is higher when the calculation unit length is larger. When using different calculation units to represent the feature index, there is a certain deviation in the peak position, which is mainly related to the selected calculation unit length. The longer the calculation unit length, the smoother the vibration amplitude curve, and the better the identification of sections with poor evenness. The smaller the calculation unit length, the clearer the vertical vibration changes during vehicle driving, and the more detailed the driving vibration situation can be reflected.

Table 2: Fitting results of V Range and IRI when the vehicle is driving at a uniform speed of 60 km/hr.

IRI (m)	10	20	30	40	50	60	70	80	90	100
R^2	0.138	0.380	0.546	0.626	0.737	0.688	0.691	0.741	0.846	0.895
a	0.068	0.112	0.145	0.150	0.157	0.149	0.158	0.173	0.185	0.181
b	1.458	0.731	0.197	0.108	−0.005	0.095	−0.050	−0.273	−0.464	−0.411

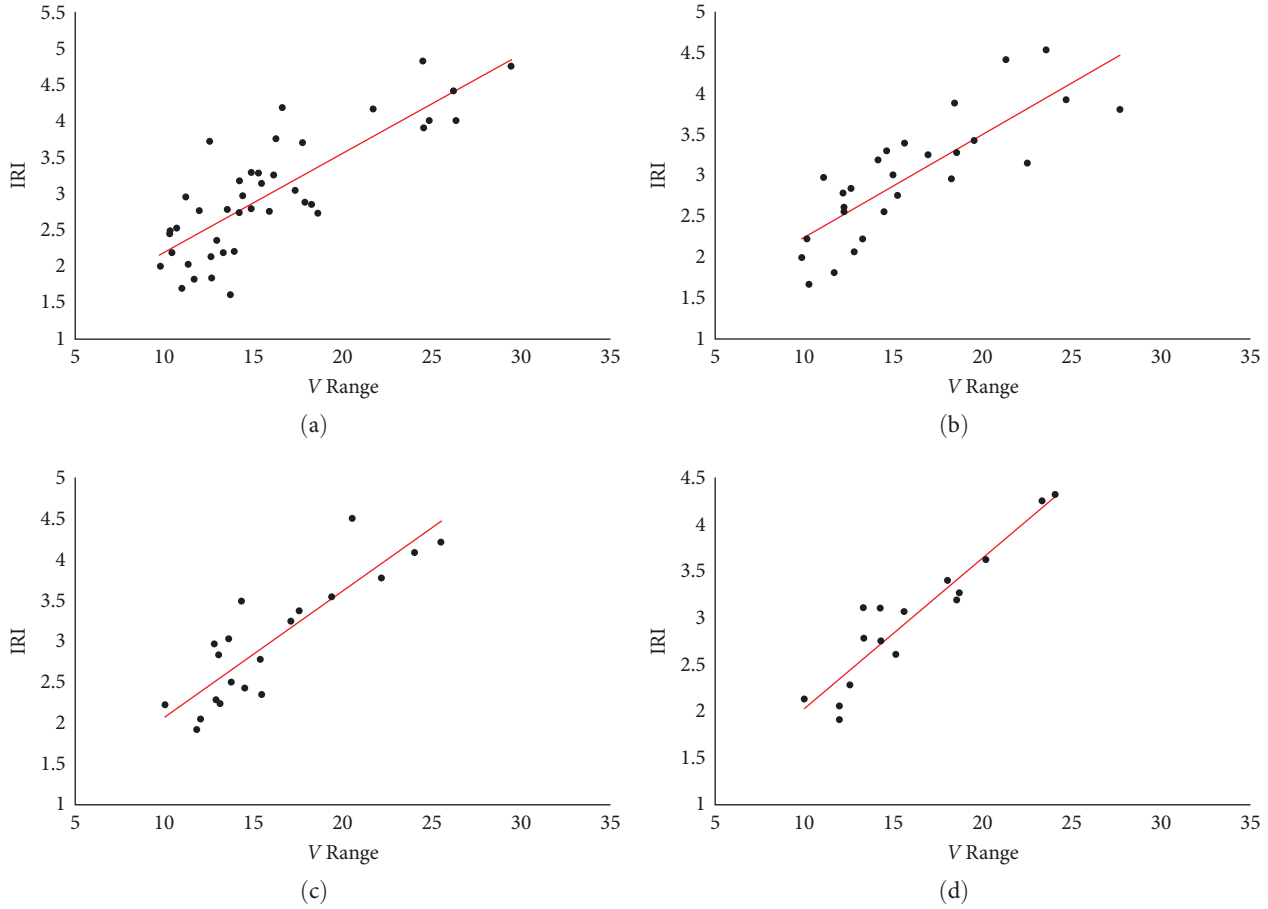

Figure 9: Fitting graph of V Range and IRI when the vehicle is driving at a uniform speed of 60 km/hr: (a) unit 40 m, (b) unit 60 m, (c) unit 80 m, and (d) unit 100 m.

3.3. Driving Vibration Feature Index and IRI Relationship Model. According to the above analysis, the pseudo-vibration velocity range (V Range) is selected as the feature index to characterize the road surface evenness (IRI). Using linear fitting, the linear relationship between V Range and IRI is established, and the IRI is calculated by testing the V Range. The linear fitting relationship between V Range and IRI corresponding to different calculation units at uniform speeds of 40 and 60 km/hr is shown in Tables 1 and 2. Here "a" represents the slope of the linear fitting formula, and "b" represents the intercept of the linear fitting formula.

The larger the calculation unit, the better the fit between V Range and IRI, and the greater the slope of the fitting curve. When the vehicle speed is uniform, the fitting degrees of 40 and 60 km/hr are similar, and the uniform driving speed within the range of 40–60 km/hr has little effect on IRI prediction. Taking the linear fitting graph at 60 km/hr as an example, as shown in Figure 9, the smaller the calculation unit, the more scattered the V Range data. As the calculation unit increases, the correlation between V Range and IRI becomes better. The best correlation is achieved when the calculation unit is 100 m, with $R^2 = 0.895$. We observed that as the interval between IRI values increases, there is an improvement in the linear fitting results. This improvement can be attributed to the larger IRI intervals effectively mitigating the measurement errors associated with smaller IRI intervals. These errors primarily arise from the challenges in time alignment during testing (where smaller distances demand higher precision in time alignment), as well as the lower redundancy in the vehicle's travel path and potential sudden incidents in smaller distances. Consequently, larger IRI intervals lead to more stable and reliable fitting outcomes.

According to the model fitting results, the driving vibration acceleration is converted into pseudo-vibration velocity,

Table 3: Fitting results for each section in 100 m unit.

Type	Road segments	R^2	a	b
Sedan	1–1	0.830	0.323	−0.020
	1–2	0.851	0.364	−0.139
	2–1	0.906	0.429	−0.472
	2–2	0.918	0.590	−1.602
	3–1	0.871	0.394	−0.210
	3–2	0.876	0.311	0.734
SUV	1–1	0.805	−0.077	0.330
	1–2	0.923	−0.100	0.346
	2–2	0.892	−1.000	0.524
	3–1	0.835	0.080	0.373

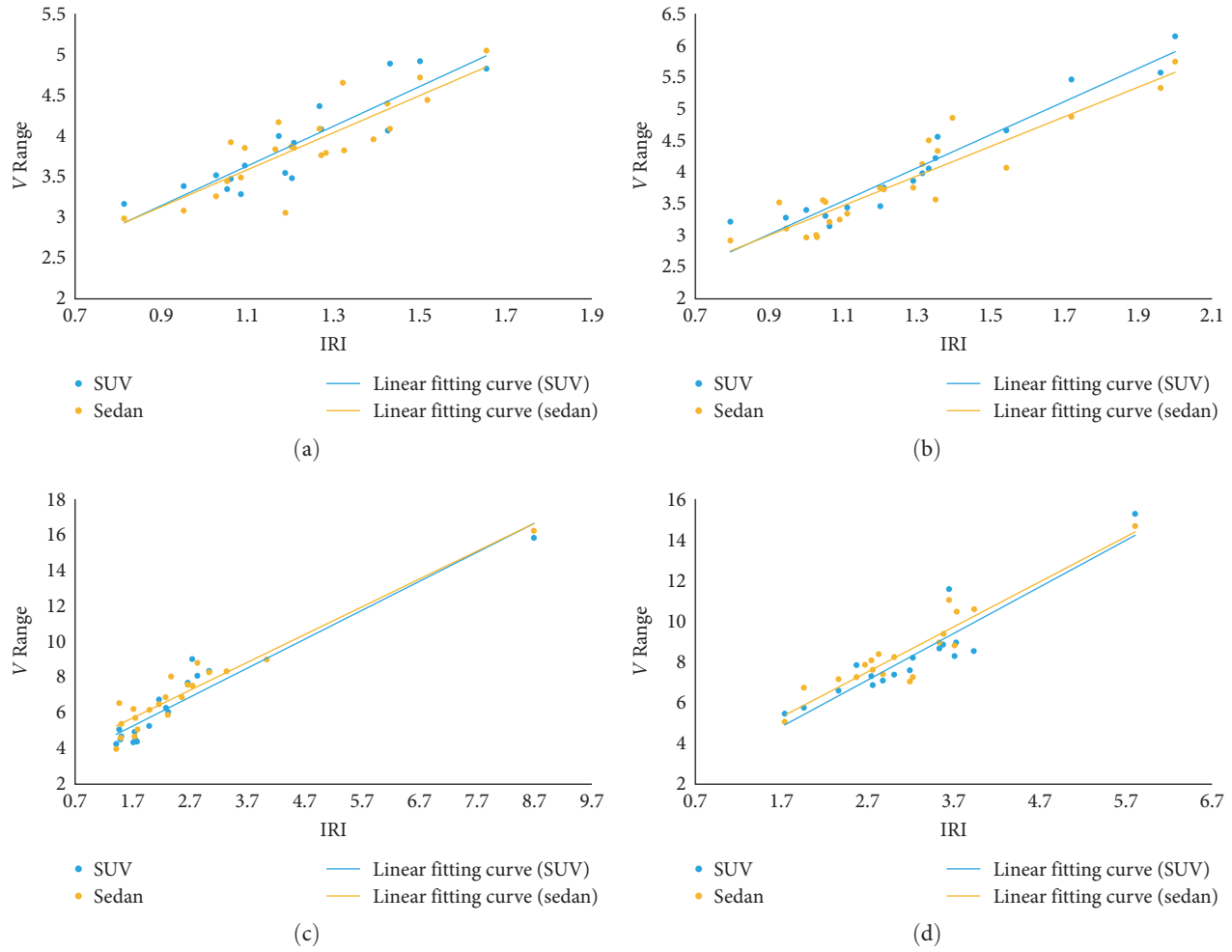

Figure 10: Fitting results for different vehicle models in 100 m unit: (a) 1–1, (b) 1–2, (c) 2–2, and (d) 3–1.

and then the range of pseudo-vibration velocity (V Range) is obtained. Through the linear fitting relationship, the road surface IRI value can be derived. To evaluate the applicability of this method under different driving conditions, the model is validated under various driving conditions.

4. Evaluation of Road Surface Evenness Based on Driving Vibration Data

4.1. Collection of Vibration Acceleration Data under Different Driving Conditions. Two vehicle models (Tesla Model 3 and Toyota RAV) were equipped with driving vibration

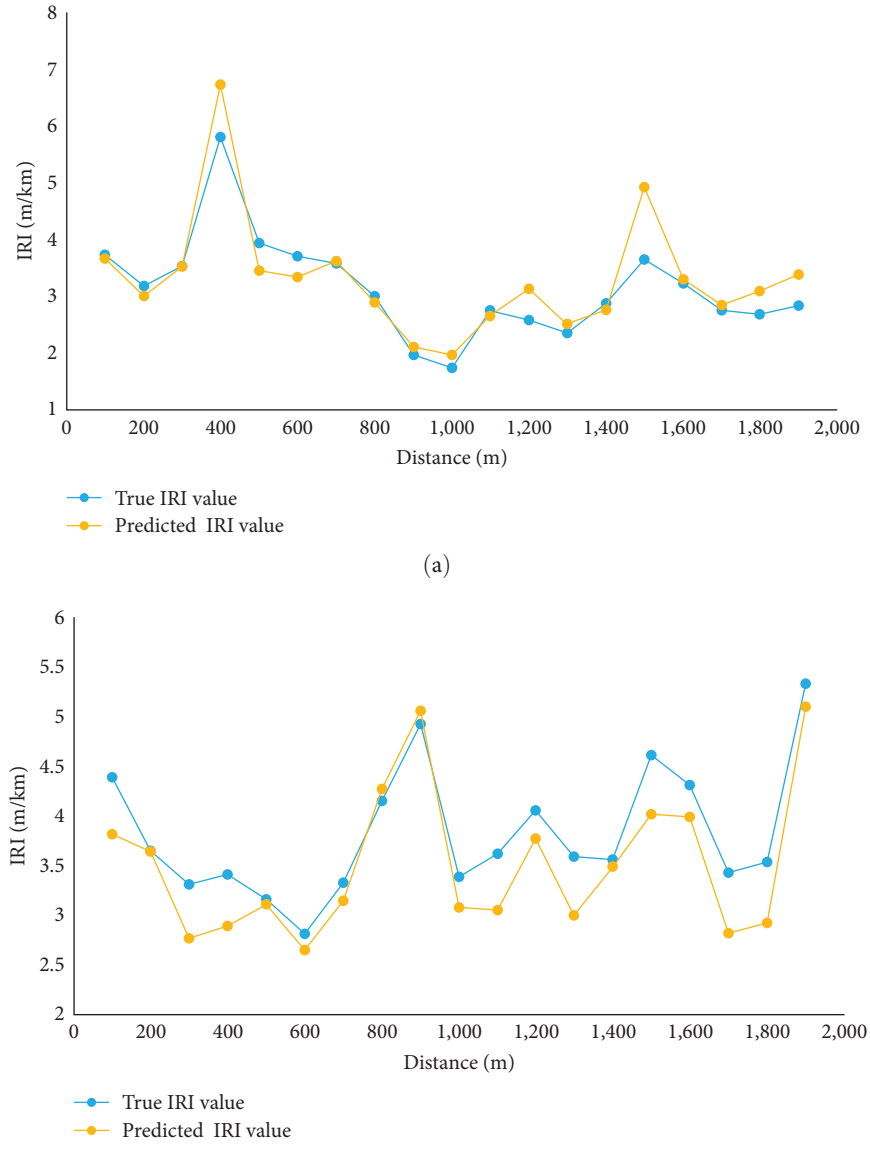

Figure 11: Test section IRI prediction. (a) Comparison of predicted and actual IRI values for SUV model on Section 3–1. (b) Comparison of predicted and actual IRI values for sedan model on Section 3–2.

acceleration data collection devices and tested on the experimental road sections that CICS vehicles had tested.

During the test, one person drove the vehicle at a constant speed of 40 km/hr, while another person in the car was responsible for operating the computer to collect data. They started recording when the vehicle reached the beginning of each test section and stopped recording when it reached the end. They also recorded the time points when the speed changed or deviated from the lane. The test sections for the sedan were the same as those for the CICS vehicles, namely 1–1, 1–2, 2–1, 2–2, 3–1, and 3–2. Due to traffic control reasons, the SUV test sections were 1–1, 1–2, 2–2, and 3–1.

4.2. Construction of IRI Relationship Model Based on Driving Vibration Acceleration Data of Different Vehicle Models. After collecting the driving vibration data, the acceleration was processed and converted into the pseudo-vibration velocity range (V Range), which was then fitted with the IRI value to establish the model. For 100 m units, the linear models for different test sections and vehicle models at a speed of 40 km/hr are shown in Table 3.

From Table 2, it can be seen that there is a certain correlation between driving vibration acceleration and IRI values. The best-fit R^2 value for the sedan can be as high as 0.91, and for the SUV, the best-fit R^2 value can be as high as 0.92. The linear fitting models for different vehicle models are shown in Figure 10.

As shown in Figure 11, the fitting trends of different vehicle models in the same section are roughly similar. The processed driving vibration acceleration data collected by different vehicle models have a good correlation with the IRI values. This proves the applicability of the model in

Table 4: Road surface unevenness IRI prediction based on driving acceleration.

Type	Speed (km/hr)	Test road segments	Fitting formula	Predictive road segments
Sedan	40	1−1, 1−2, 2−1, 2−2, 3−1	$y = 0.3745x - 0.2069$	3–2
SUV	40	1−1, 1−2, 2−2	$y = 0.4853x - 0.6834$	3–1

different vehicle models and demonstrates the feasibility of using pseudo-vibration acceleration range for road surface evenness prediction.

4.3. Road Surface Evenness Prediction Based on Driving Vibration Data. Using the established relationship models between driving vibration acceleration and IRI values for different vehicle models, IRI value predictions for the test sections were performed. In the fitting equation, Y represents IRI100 m and X represents V Range, as shown in Table 4. The prediction results are shown in Figure 11.

As shown in Figure 11, the road surface evenness values predicted by the linear fitting model are in good agreement with the actual values. The average relative error between the IRI predicted values and the actual values for the SUV test is 6.7%, and the average relative error between the IRI predicted values and the actual values for the sedan test is 8.9%. An error accuracy within 10% can meet the testing requirements for low-grade road surface IRI values.

5. Conclusion

This paper demonstrates the feasibility of using driving vibration acceleration data collection devices to detect road surface evenness. It derives and establishes the relationship between driving vibration acceleration data and the IRI, obtaining road surface evenness evaluation results based on acceleration. The main research findings are as follows:

(1) Developed a driving vibration acceleration data collection device that synchronizes the collection of acceleration, speed, and GPS data. By processing and extracting the feature values of driving acceleration data on the test sections, the acceleration data are innovatively converted into pseudo-vibration data.

(2) For different calculation unit elements, the optimal fitting result is obtained with the range index corresponding to the pseudo-vibration velocity and the IRI. As the calculation unit element increases, the range and IRI linear fitting results improve, and the fitting curve slope also increases. However, when the calculation unit element is 100 m, the fitting degree is greater than 0.8.

(3) Using the pseudo-vibration velocity range as the feature index representing the road surface evenness IRI value, linear fitting is performed. At 40 and 60 km/hr uniform speeds, the correlation between the pseudo-velocity range within the 100 m section and the IRI value reaches 0.8706 and 0.8960, respectively. The fitting degrees at 40 and 60 km/hr are similar, and the influence of uniform driving speed within the 40–60 km/hr range on IRI prediction is not significant.

(4) Testing with different vehicle models showed that the pseudo-velocity range and IRI relationship model is applicable to both sedans and SUVs, with similar fitting trends and small fluctuation ranges for V Range values. The relative error for the sedan evenness testing model is 8.9%, and for the SUV evenness testing model, it is 6.7%.

This study developed a road surface evenness detection method based on driving vibration acceleration data collection devices. Further research will extend the model's application to more vehicle types (such as, buses, taxis, etc.), and achieve real-time monitoring and integration with intelligent transportation systems and intelligent maintenance platforms to improve the efficiency of road surface evenness testing.

In the future, further improvements can be made by enhancing the accuracy of both the accelerometer and GPS sensors, thereby increasing the precision of road surface IRI detection. By developing advanced data processing algorithms, such as neural network models, the acceleration data can be utilized more effectively for IRI value detection. Additionally, these models need to be adjusted and tested for different environmental conditions, road surface types, and vehicle types to ensure their broad applicability and reliability.

Data Availability

The data presented in this study are available upon request from the corresponding author.

Conflicts of Interest

The authors declare that they have no conflicts of interest.

Authors' Contributions

Hongwei Jiang contributed to conceptualization. Yanhong Zhang contributed to validation. Xinlong Tong contributed to writing—review and editing. Yinghao Miao contributed to methodology. Zhoujing Ye contributed to formal analysis. Junqing Li and Yu Wang contributed to investigation. Yanhong Zhang and Zhoujing Ye contributed to writing—original draft preparation. All authors have read and agreed to the published version of the manuscript.

Acknowledgments

The authors would like to express their thanks to everyone who offered help and advice in the creation of the paper. This paper is supported by the project "Research and Development of Highway Intelligent Detection Technology and Vehicle-Mounted Platform Based on Ubiquitous Sensing"

and "Pilot Application of Highway Whole Life Cycle Maintenance Decision-Making Based on Ubiquitous Perception."

References

[1] J. Zhang, L. Gao, and Z. Dong, "Review on materials and technology of multifunctional maintenance of asphalt pavement," *Journal of Municipal Technology*, vol. 41, no. 10, pp. 80–93, 2023.

[2] Z. Wang, "A novel unsupervised clustering algorithm for monitoring and evaluating bridge structural health," *Journal of Municipal Technology*, vol. 42, no. 1, pp. 68–72, 2024.

[3] K. Urano, K. Hiroi, S. Kato, N. Komagata, and N. Kawaguchi, "Road surface condition inspection using a laser scanner mounted on an autonomous driving car," in *2019 IEEE International Conference on Pervasive Computing and Communications Workshops (PerCom Workshops)*, pp. 826–831, IEEE, Kyoto, Japan, 2019.

[4] X. Lu and X. Qian, "Prediction method of pavement roughness by XGBoost," *Journal of Municipal Technology*, vol. 41, no. 6, pp. 10–14, 2023.

[5] X. Ma, Q. Liu, and J. Wu, "Research on pavement roughness prediction and model interpretation based on machine learning methods," *Journal of Municipal Technology*, vol. 41, no. 8, pp. 39–44, 2023.

[6] C. R. Bennett, *Establishing Reference Transverse Profiles for Rut Depth Measurements in New Zealand*, Data Collection Limited, Motueka, New Zealand, 2002.

[7] X. Song, "Research on dynamic response characteristics of the shield tunnel under traffic dynamic load of urban road," *Journal of Municipal Technology*, vol. 41, no. 9, pp. 88–95, 2023.

[8] Y. Zhuo and H. Chen, "Analysis of pedestrian-induced vibration and design of TMD damping for footbridge," *Journal of Municipal Technology*, vol. 41, no. 11, pp. 1–8, 2023.

[9] K. Tomiyama and A. Kawamura, "Application of lifting wavelet transform for pavement surface monitoring by use of a mobile profilometer," *International Journal of Pavement Research and Technology*, vol. 9, no. 5, pp. 345–353, 2016.

[10] K. Chen, M. Lu, X. Fan, M. Wei, and J. Wu, "Road condition monitoring using on-board three-axis accelerometer and GPS sensor," in *6th International ICST Conference on Communications and Networking in China (CHINACOM)*, pp. 1032–1037, IEEE, Harbin, 2011.

[11] R. Brunauer and K. Rehrl, "Supporting road maintenance with in-vehicle data: results from a field trial on road surface condition monitoring," in *2016 IEEE 19th International Conference on Intelligent Transportation Systems (ITSC)*, pp. 2236–2241, IEEE, Rio de Janeiro, Brazil, 2016.

[12] J. Zhang, L. Wang, T. Zhou, and Y. Wu, "Research on intelligent detection method of road surface evenness based on driving vibration," *China Foreign Highway*, vol. 40, pp. 31–36, 2020.

[13] A. Chatterjee and Y. C. Tsai, "Training and testing of smartphone-based pavement condition estimation models using 3d pavement data," *Journal of Computing in Civil Engineering*, vol. 34, no. 6, Article ID 04020043, 2020.

[14] A. Zhang, K. C. P. Wang, B. Li et al., "Automated pixel-level pavement crack detection on 3D asphalt surfaces using a deep-learning network," *Computer-Aided Civil and Infrastructure Engineering*, vol. 32, no. 10, pp. 805–819, 2017.

[15] A. A. Elhadidy, S. M. El-Badawy, and E. E. Elbeltagi, "A simplified pavement condition index regression model for pavement evaluation[J]," *International Journal of Pavement Engineering*, vol. 22, no. 5, pp. 643–652, 2021.

[16] W. Aleadelat and K. Ksaibati, "Estimation of pavement serviceability index through android-based smartphone application for local roads," *Transportation Research Record*, vol. 2639, no. 1, pp. 129–135, 2017.

[17] M. Hafez, K. Ksaibati, and R. Anderson-Sprecher, "Utilizing statistical techniques in estimating uncollected pavement-condition data," *Journal of Transportation Engineering*, vol. 142, no. 12, Article ID 04016065, 2016.

[18] K. Zang, J. Shen, H. Huang, M. Wan, and J. Shi, "Assessing and mapping of road surface roughness based on GPS and accelerometer sensors on bicycle-mounted smartphones," *Sensors*, vol. 18, no. 3, Article ID 914, 2018.

[19] P. Mohan, V. N. Padmanabhan, and R. Ramjee, "Nericell: rich monitoring of road and traffic conditions using mobile smartphones," in *Proceedings of the 6th ACM Conference on Embedded Network Sensor Systems*, pp. 323–336, ACM, 2008.

[20] L. Forslof, "Roadroid-smartphone road quality monitoring," 19th ITS World Congress ERTICO-ITS EuropeEuropean CommissionITS AmericaITS Asia-Pacific, 2012.

[21] G. Alessandroni, L. C. Klopfenstein, S. Delpriori et al., "Smartroadsense: collaborative road surface condition monitoring," in *Proceedings of the UBICOMM*, pp. 210–215, 2014.

[22] N. Abdelaziz, R. T. Abd El-Hakim, S. M. El-Badawy, and H. A. Afify, "International roughness index prediction model for flexible pavements," *International Journal of Pavement Engineering*, vol. 21, no. 1, pp. 88–99, 2020.

[23] Z. Zhang, H. Zhang, S. Xu, and W. Lv, "Pavement roughness evaluation method based on the theoretical relationship between acceleration measured by smartphone and IRI," *International Journal of Pavement Engineering*, vol. 23, no. 9, pp. 3082–3098, 2022.

[24] J. Xu and X. Yu, "Pavement roughness grade recognition based on one-dimensional residual convolutional neural network," *Sensors*, vol. 23, no. 4, Article ID 2271, 2023.

[25] V. Douangphachanh and H. Oneyama, "Using smartphones to estimate road pavement condition," in *Proceedings of the International Symposium for Next Generation Infrastructure*, University of Wollongong, Australia, 2013, October.

[26] D. Bisconsini, J. Y. M. Núñez, R. Nicoletti, and J. L. F. Júnior, "Pavement roughness evaluation with smartphones," *International Journal of Science and Engineering Investigations*, vol. 7, no. 72, pp. 43–52, 2018.

[27] W. Aleadelat, K. Ksaibati, C. H. G. Wright, and P. Saha, "Evaluation of pavement roughness using an android-based smartphone," *Journal of Transportation Engineering, Part B: Pavements*, vol. 144, no. 3, Article ID 04018033, 2018.

[28] Y. I. Alatoom and T. I. Obaidat, "Measurement of street pavement roughness in urban areas using smartphone," *International Journal of Pavement Research and Technology*, vol. 15, pp. 1003–1020, 2022.

[29] A. Aboah and Y. Adu-Gyamfi, "Smartphone-based pavement roughness estimation using deep learning with entity embedding," *Advances in Data Science and Adaptive Analysis*, vol. 12, no. 3n04, Article ID 2050007, 2020.

[30] R. M. K. Sandamal and H. R. Pasindu, "Applicability of smartphone-based roughness data for rural road pavement condition evaluation," *International Journal of Pavement Engineering*, vol. 23, no. 3, pp. 663–672, 2022.

[31] S. Z. Xu, "Research on pavement smoothness prediction based on intelligent algorithm," AnHui University of Science and Technology, A Dissertation in Architecture and Civil Engineering, 2022.

[32] M. A. Bidgoli, A. Golroo, H. S. Nadjar, A. G. Rashidabad, and M. R. Ganji, "Road roughness measurement using a cost-effective sensor-based monitoring system," *Automation in Construction*, vol. 104, pp. 140–152, 2019.

[33] Z. Du, W. R. Zhang, and X. Y. Zhu, "Road roughness assessment based on fusion of connected-vehicles data," *China Journal of Highway and Transport*, pp. 1–26, 2023.